Medical Engineering and Physics 000 (2018) 1–7

Contents lists available at ScienceDirect

Medical Engineering and Physics

journal homepage: www.elsevier.com/locate/medengphy

Biomechanical characteristics of immediately loaded and osseointegration dental implants inserted into Sika deer antler

Yun He[a,b], Istabrak Hasan[b,c,*], Ludger Keilig[b,c], Dominik Fischer[d,e], Luisa Ziegler[e], Markus Abboud[g], Gerhard Wahl[f], Christoph Bourauel[b]

[a] Orofacial Reconstruction and Regeneration Laboratory, Department of Oral and Maxillofacial Surgery, the Hospital of Stomatology, Southwest Medical University, Luzhou, China
[b] Oral Technology, Dental School, University of Bonn, Welschnonnenstr. 17, 53111 Bonn, Germany
[c] Department of Prosthetic Dentistry, Preclinical Education and Materials Science, Dental School, University of Bonn, Bonn, Germany
[d] Raptor Center and Wildlife Parc Hellenthal, Hellenthal, Germany
[e] Clinic for Birds, Reptiles, Amphibians and Fish, Veterinary Faculty, Justus Liebig University Giessen, Giessen, Germany
[f] Department of Oral Surgery, Dental School, University of Bonn, Bonn, Germany
[g] Department of Prosthodontics and Digital Technology, School of Dental Medicine, Stony Brook University, 1104 Westchester Hall, Stony Brook, New York

ARTICLE INFO

Article history:
Received 30 September 2017
Revised 13 March 2018
Accepted 16 April 2018
Available online xxx

Keywords:
Implant
Sika deer antler
Immediate loading
Osseointegration
Stress

ABSTRACT

This study aimed to compare biomechanical characteristics of immediately loaded (IL) and osseointegrated (OS) dental implants inserted into Sika deer antler and lay a foundation for developing an alternative animal model for dental implants studies. Two implants per antler were inserted. One implant was loaded immediately via a self-developed loading device; the other was submerged and unloaded as control. IL implants were harvested after different loading periods. The unloaded implants were collected after OS and the shedding of antler. Specimens were scanned by μCT scanner and finite element models were generated. A vertical force of 10 N was applied on the implant. The mean values of maximum displacements, stresses and strains were compared. The results showed that the density of antler tissue around the implants dramatically increased as the loading time increased. After shedding the antler, 3 pairs of antlers were collected and the density of antler tissue remained in a similar value in all specimens. The maximum values of displacement and stresses in implant and stresses and strains in antler tissue were significantly different among OS models. In one antler, all the biomechanical parameters of IL model were significantly higher than those of OS model of the same animal ($P < 0.05$) and wider distributions were obtained from IL model. It can be concluded that implants inserted into Sika deer antler might not disturb the growth and calcification process of antler and the use of Sika deer antler model is a promising alternative for implant studies that does not require animal sacrifice.

1. Introduction

With the worldwide growing of aging population, there has been considerable increase in the demand for the replacement of lost teeth by means of implant-retained restorations over the last few decades. The clinical success of implant therapy is based on osseointegration, defined as the direct contact between living bone and the implant without the interposition of fibrous tissue [1–3]. Conventionally, loading on implant-retained restoration should be avoided before osseointegration. However, immediately loaded (IL) implants which allow for shorter rehabilitation times have shown similar implant stability and success rate compared with traditional delayed loading implants. Some studies showed that IL is beneficial to delayed loading, since loading is capable of stimulating the healing process [4–6]. IL implants appear to increase patient satisfaction and avoid the difficulty of wearing a conventional temporary restoration during the healing phase as well [7]. Thus, there is a trend in using an immediate loading protocol for implant-retained restoration currently.

While animal models closely represent the mechanical and physiological human clinical situation, they have been widely used in investigating dental implants in loaded or unloaded situations over potentially long time spans and in different tissue qualities (e.g., normal healthy or osteoporotic bone) and ages [8]. Each animal model has unique advantages and disadvantages; therefore for

* Corresponding author at: Oral Technology, Department of Prosthetic Dentistry, Preclinical Education and Materials Science, Dental School, University of Bonn, Welschnonnenstr. 17, 53111 Bonn, Germany.
E-mail address: ihasan@uni-bonn.de (I. Hasan).

https://doi.org/10.1016/j.medengphy.2018.04.021
1350-4533/

different purposes there are numerous models for testing the properties of implant and its surrounding tissue in vivo. Specifically, for studies investigating bone remodeling process around IL implants, the animal model should have similar bone characteristics to human bone and be appropriate for inserting implants and applying loadings [9]. However, the main disadvantages for the existing animal models are the uncontrolled loads that are exerted on the implants and the sacrificed fate of animals. For these reasons, exploring a novel animal model that is able to apply a controlled force on the inserted IL implant and does not interfere with the animals' behavior is admirable.

Deer are the only mammals that are capable of fully regenerating a complex organ, called antlers [10]. The ability to fully regenerate stands out as the most impressive feature of antlers. The repeated regeneration each year is even more remarkable, because mammalian appendages are generally considered as being incapable of regeneration. Deer antlers grow annually in defiance of what could be considered nature's rules [11]. The annual cycle of antler growth starts in spring. After the rapid elongation and the formation of lateral branches in summer, antler gradually becomes calcified in late summer or autumn. The process of calcification is initiated from the base of the antler and proceeds up through the antler and finishes when the distal ends of the tines form sharp tips [11]. After the calcification process has been completed, in conjunction with the loss of blood vessels and nerves, the velvet skin is shed. In winter, the bare bony antlers are firmly attached to the living pedicle and are not "cast" until the following spring. Antler casting triggers another round of antler regeneration [12]. This cycle provides a relative reasonable time span for investigating bone remodeling processes around implants inserted into the antler without sacrificing the animal. Besides, deer antlers are similar to human bones in regard to chemical composition and physiological structure [13,14]. Furthermore, as a muscle- and joint-free bony cranial appendage [15,16], antlers provide a fascinating model to investigate bone remodeling process around IL implant without the influence of external forces (except for gravity).

The primary aim of this study was to compare bone remodeling and biomechanical characteristics of immediately loaded and osseointegrated dental implants inserted into Sika deer antler. Secondly, the aim was to lay a theoretical foundation for developing an alternative animal model for studying bone remodelling around dental implants.

2. Materials and methods

2.1. Animal welfare statement

All animals were handled according to the policies and principles established by the German animal welfare act (TSchG, last amended on 3rd December 2015), approved by the North Rhine-Westphalia State Agency for Nature, Environment and Consumer Protection as competent authority (Permission No.: LANUV NRW, 84-02.04.2014.A462).

2.2. Surgery procedure

In July of 2015, six 4-year-old male Sika deer (bred at Wildlife Parc Hellenthal, Germany) were anesthetized using 1.2–1.5 ml Hellabrunn's mixture (100 mg Ketamine and 125 mg Xylazine per ml) according to standard procedures [17,18]. After disinfection and additional local anaesthesia with 3–5 ml lidocaine (Lidocain B. Braun 2%, B. Braun Melsungen, Melsungen, Germany), a longitudinal incision was performed and velvet flap elevated. Implant site was prepared at a position near a branching of the antler by sequential drilling under sterile saline irrigation according to the surgical protocol. Two implants per antler were inserted in a distance of 2.5 cm. The implants were Straumann Roxolid® soft tissue level implants (Institut Straumann AG, Basel, Switzerland) with a length of 10 mm and a diameter of 3.3 mm. After suturing the incision, the most proximal implant was vertically loaded immediately via a self-developed screw retained loading device [19], while the other one remained unloaded as a control. The motor of the control electronics were fixed on the other antler by colored bandages. Bandage with the different colors, blue, orange, yellow, red and black were used to distinguish the animals (Fig. 1). One deer was dead during the anesthetisation phase. After 2, 3, 4, 5 and 6 weeks, respectively, the loaded implants and surrounding tissue were randomly taken out with a trephine from one animal and the wounds were filled with bone wax (Ethicon®-bone wax, Johnson and Johnson, Hamburg, Germany), sutured and bandage protected. The samples were fixed in buffered formalin (4%). The unloaded implants remained in the antler for osseointegration. In winter, the antlers were collected after their shedding. Finally only three pairs of antlers, blue, orange and black, were able to be collected. The other two pairs of antlers could not be found. Thereafter, the unloaded implant with surrounding antler tissue and the antler tissue adjacent to the former specimen were sectioned for further investigation.

2.3. Numerical analysis

Specimens were prepared and scanned in a µCT scanner (SkyScan 1174, Bruker-micro CT, Kontich, Belgium) using 50 kV and 800 μA, rotation step of 0.25°. Data sets were reconstructed. After scanning the sample, calibration phantom with known density of calcium hydroxyapatite (SkyScan 1174, Bruker-microCT, Kontich, Belgium) was scanned on the same day by using the same parameters. Bone mineral density (BMD) of antler tissue (including cortical and trabecular bone) was calculated by using Bruker-Micro CT-Analyser (Bruker-micro CT, Kontich, Belgium).

µCT data of the specimens with implant were imported into Mimics research 18.0 (Materialise NV, Leuven, Belgium). Later on, three masks were created by defining different Hounsfield range, including the mask of implant, antler tissue (including cortical bone and trabecular bone) and bone marrow. After reconstruction, data were further processed in 3-Matic research 10.0 (Materialise NV, Leuven, Belgium) and converted into 3D finite element (FE) models using 4-noded tetrahedral elements. The final models of unloaded implant consisted of 532,709; 1,116,651; and 819,677 elements in specimens of blue, orange and black antler, respectively (Fig. 2). The 3D FE analysis was performed using the software package MSC.Marc/Mentat 2010 (MSC. Software, Santa Ana, CA, USA).

All materials were assumed to be isotropic and linear elastic. Young's modulus of the antler tissue was calculated by using the formula [20]:

$$E = \begin{cases} 2014\rho^{2.5} \ if \ \rho \le 1.25 \ g/cm^3 \\ 1763\rho^{3.2} \ if \ \rho > 1.25 \ g/cm^3 \end{cases}$$

Material properties of the implant (Roxolid® material) and bone marrow that were used in the analysis were taken from the literature (Table 2) [21,22].

Friction contact (frictional coefficient $\mu = 0.3$) was defined between antler tissue and implant for IL models. Osseointegrated condition was simulated between antler tissue and implant for unloaded (OS) models.

All models were constrained in all directions at the nodes on the lateral sides and bottom of the antler segment. Analog to the loading behavior of the implants in deer antler, a vertical force of 10 N, was applied onto the implant. In the regions of maximum

Please cite this article as: Y. He et al., Biomechanical characteristics of immediately loaded and osseointegration dental implants inserted into Sika deer antler, Medical Engineering and Physics (2018), https://doi.org/10.1016/j.medengphy.2018.04.021

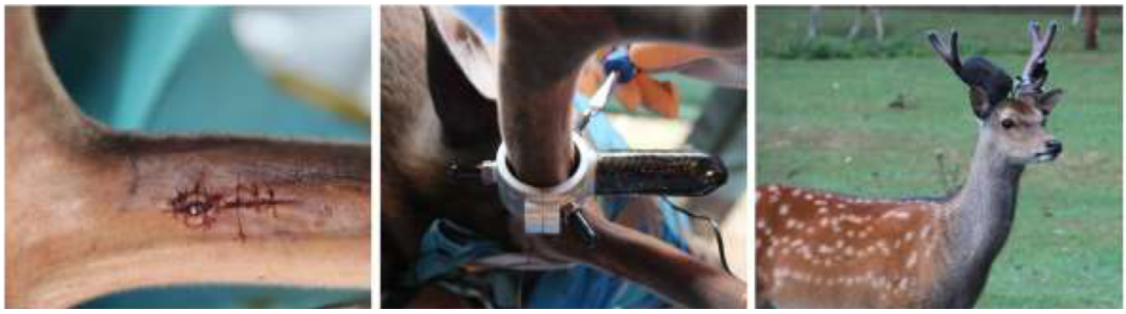

Fig. 1. Each animal received two implants at a position near a branching of the antler (left). One of the implants was loaded by an autonomous loading device, and the second one was submerged and remained unloaded (middle). An example of colored bandage (black) was used to fix the motor of the lading device (right).

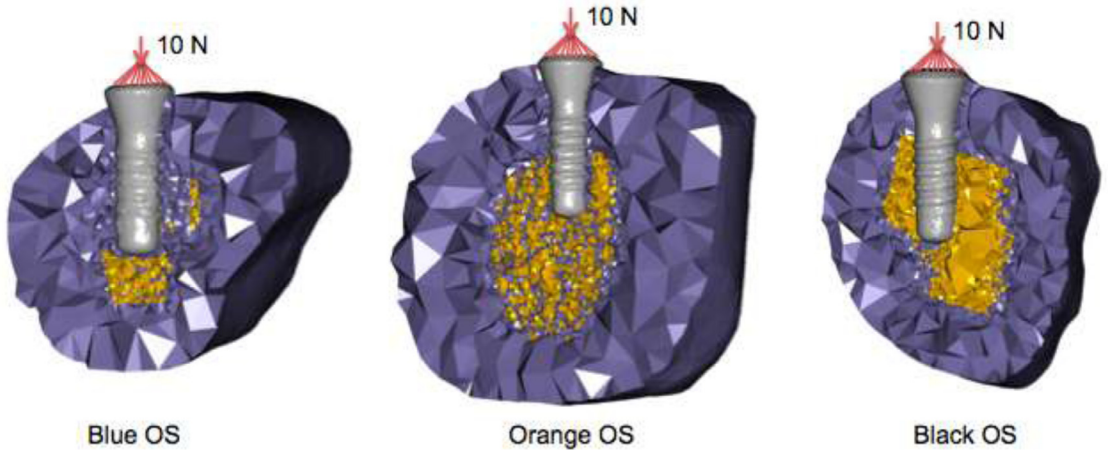

Fig. 2. Finite element models of blue, orange, and black Sika deer antler segments.
Grey: implant; blue: original antler tissue around the implant in the samples; yellow: bone marrow.

displacements, stresses and strains, ten nodes were randomly selected and the values were recorded respectively. The mean values of ten nodes were recorded as mean ± standard deviation (SD) and compared.

2.4. Statistical evaluation

Data were analysed using IBM SPSS Statistics for Windows, version 20.0 software (IBM Corp., Armonk, NY, USA). One way ANOVA with the SNK comparison test was used to explore the differences of displacements, stresses and strains among different osseointegration specimens. Independent Samples *t*-test was used to compare the differences of displacements, stresses and strains between the two IL specimens. The biomechanical values of OS and IL specimens in the same animal were compared using paired *t*-test. A significance level of 0.05 was chosen.

3. Results

3.1. BMD and Young's modulus of the antler tissue

Deer with blue, orange, yellow, red and black bandage, respectively, received 2, 3, 4, 5, 6 weeks immediately loading. As the loading time increased, BMD of antler tissue surrounding the implant dramatically increased. After shedding the antler, the BMD of antler tissue in specimens with osseointegrated implants (blue: 1.09 g/cm^3, orange: 1.26 g/cm^3, black: 1.30 g/cm^3) and without implants (blue: 1.28 g/cm^3, orange: 1.20 g/cm^3, black: 1.31 g/cm^3) were in a similar range. For orange antler, the BMD of antler tissue around OS implant was higher than that around IL implant.

Table 1
Bone mineral density (BMD, g/cm^3) of the antler tissue around implants at different healing periods.

Deer antler	Specimen		
	IL	OS with implant	OS without implant
Blue (2-week)	–	1.09 ± 0.24	1.28 ± 0.18
Orange (3-week)	0.31 ± 0.01	1.26 ± 0.17	1.20 ± 0.12
Yellow (4-week)	0.92 ± 0.23	–	–
Red (5-week)	1.54 ± 0.40	–	–
Black (6-week)	2.00 ± 0.53	1.30 ± 0.11	1.31 ± 0.13

IL: Immediately loaded implant specimen, OS with implant: Osseointegration implant specimen, OS without implant: The specimen of antler tissue without implant adjacent to the osseointegration implant specimen.

Table 2
Material properties of the numerical models.

Material	Young's modulus (MPa)	Poisson ratio
Blue Antler tissue (OS)	2487	0.30
Orange Antler tissue (3-week IL)	108	0.30
Orange Antler tissue (OS)	3665	0.30
Black Antler tissue (6-week IL)	16,200	0.30
Black Antler tissue (OS)	4092	0.30
Roxolid®	98,000	0.30
Bone marrow	2	0.16

Interestingly, in black antler the BMD of antler tissue around IL implant (2.00 g/cm^3) was much higher than that around OS implant (1.30 g/cm^3). The BMD of specimens and corresponding material properties of the numerical models were shown in Tables 1 and 2.

Please cite this article as: Y. He et al., Biomechanical characteristics of immediately loaded and osseointegration dental implants inserted into Sika deer antler, Medical Engineering and Physics (2018), https://doi.org/10.1016/j.medengphy.2018.04.021

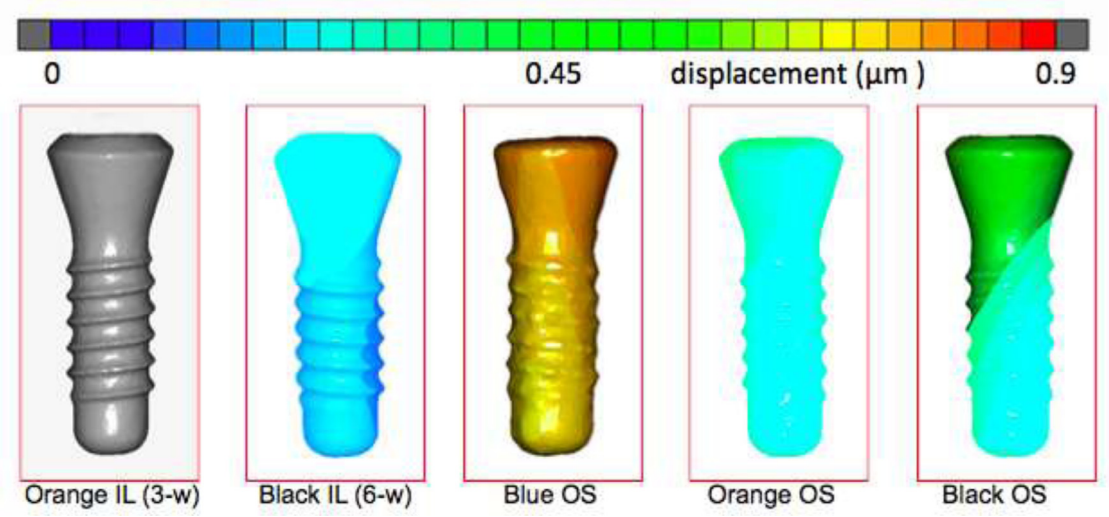

Fig. 3. Stress distributions in implant for IL-models and OS-models. Orange IL (3-w): model of orange antler with immediately loaded implant for 3 weeks; black IL (6-w): model of black antler with immediately loaded implant for 6 weeks; blue OS: model of blue antler with unloaded implant; orange OS: model of orange antler with unloaded implant; black OS: model of black antler with unloaded implant.

Table 3
Obtained maximum values of displacements (μm) in implants in immediate loading (IL) and osseointegrated (OS) models with different postoperative time.

	IL	OS	*t*	*P* value
Blue (2-week)	–	0.9 ± 0.1		
Orange (3-week)	6.2 ± 0.3	0.5 ± 0.1[a]	57.3	<0.001
Black (6-week)	0.4 ± 0.1	0.6 ± 0.1[a,b]	−2.9	0.018
F/*t*	59.6	55.2	–	–
P value	<0.001	<0.001		

[a] $P < 0.05$, when compared with blue.
[b] $P < 0.05$, when compared with orange.

Table 4
Obtained maximum values of stresses in implant (MPa) in immediate loading (IL) and osseointegrated (OS) models in different postoperative time.

	IL	OS	*t*	*P* value
Blue (2-week)	–	1.0 ± 0.1		
Orange (3-week)	2.8 ± 0.1	1.2 ± 0.1[a]	29.6	<0.001
Black (6-week)	2.5 ± 0.0	0.9 ± 0.1[b]	62.3	<0.001
F/*t*	11.7	10.0	–	–
P value	<0.001	0.001		

[a] $P < 0.05$, when compared with blue.
[b] $P < 0.05$, when compared with orange.

3.2. FE results

The differences of maximum displacement of implants were significant among the three OS models (Table 3). The highest and lowest values in OS samples were observed with blue antler (0.9 μm) and orange antler models (0.5 μm). The maximum displacement of the implant in orange antler IL model was significantly higher than that in orange antler OS model ($P < 0.05$). Conversely, in black antler models significant higher values were obtained in OS model compared with IL model ($P < 0.05$).

Stresses in the implant were significantly different among the OS models (Table 4), and the distribution was concentrated in the neck of implant. The highest values of stresses in the implant were observed in OS models (1.2 MPa) and wider distribution was founded in orange antler model (Fig. 3). There were no significant differences between blue and black antler OS models ($P > 0.05$). Both for orange and black antler models, the maximum stresses of the implant in IL models were significantly higher than that in OS models ($P < 0.05$). The distribution of IL models was wider than that of OS models.

Table 5
Obtained maximum values of stresses (MPa) in antler tissue in osseointegrated (OS) and immediate loading (IL) models with different postoperative time.

	IL	OS	*t*	*P* value
Blue (2-week)		1.0 ± 0.1		
Orange (3-week)	2.4 ± 0.8	1.1 ± 0.1[a]	4.9	0.001
Black (6-week)	6.5 ± 1.5	1.3 ± 0.2[a]	10.7	<0.001
F/*t*	−7.5	7.9	–	–
P value	<0.001	0.002		

[a] $P < 0.05$, when compared with blue.

The stress in antler tissue was increased from 2.4 MPa (3 weeks after IL) to 6.5 MPa (5 weeks after IL) in IL models. Stresses in antler tissue were considerably different among OS models, and the distribution was similarly concentrated in the antler tissue around the neck of implant (Table 5, Fig. 4). For OS models, the highest and lowest values of maximum stresses in antler tissue were observed in black antler (1.3 MPa) and blue antler models (1.0 MPa). Both for orange and black antler models, the maximum stresses in antler tissue in IL models were significantly higher than that in OS models ($P < 0.05$).

Maximum strain in antler tissues was decreased from 9879 μstrain to 363 μstrain during the healing time for the IL models. Among OS models, the highest values of strains in antler tissue were detected in blue antler OS model (1888 μstrain), followed by orange antler (686 μstrain) and black antler OS models (523 μstrain). The blue antler OS model also showed the widest distribution of strains in antler tissue. The differences among them were significant ($P < 0.05$). For orange antler models, the maximum strains in antler tissue in IL models were significantly higher than that in OS models ($P < 0.05$). In contrast, the opposite results were obtained in black antler models (Table 6, Fig. 6).

4. Discussion

Studies indicated that implant loading can be performed immediately or early after insertion without disturbing the biological osseointegration process and can be beneficial for peri-implant bone

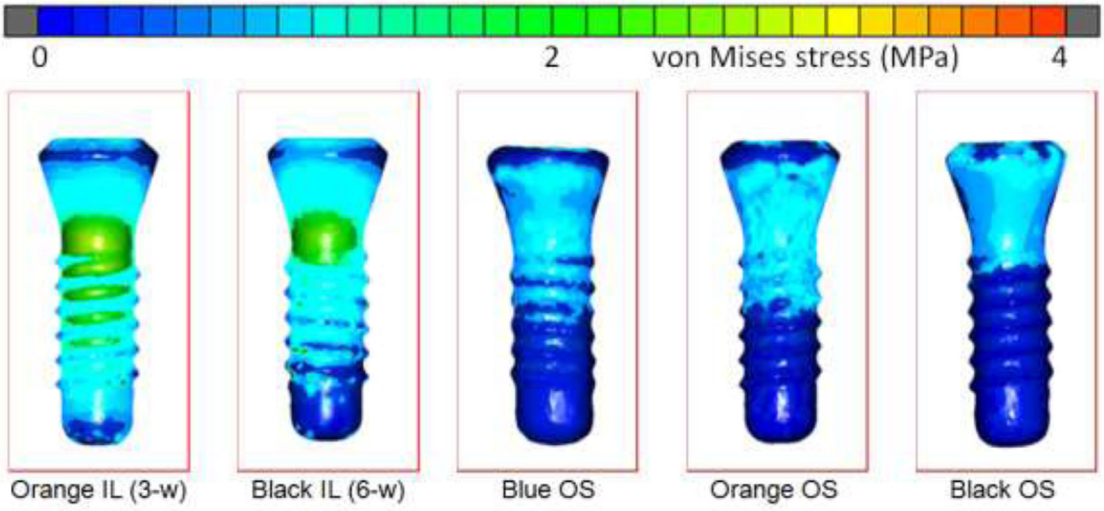

Fig. 4. Stress distributions in the antler tissue for IL-models and OS-models. Orange IL (3-w): model of orange antler with immediately loaded implant for 3 weeks; black IL (6-w): model of black antler with immediately loaded implant for 6 weeks; blue OS: model of blue antler with unloaded implant; orange OS: model of orange antler with unloaded implant; black OS: model of black antler with unloaded implant.

implant.

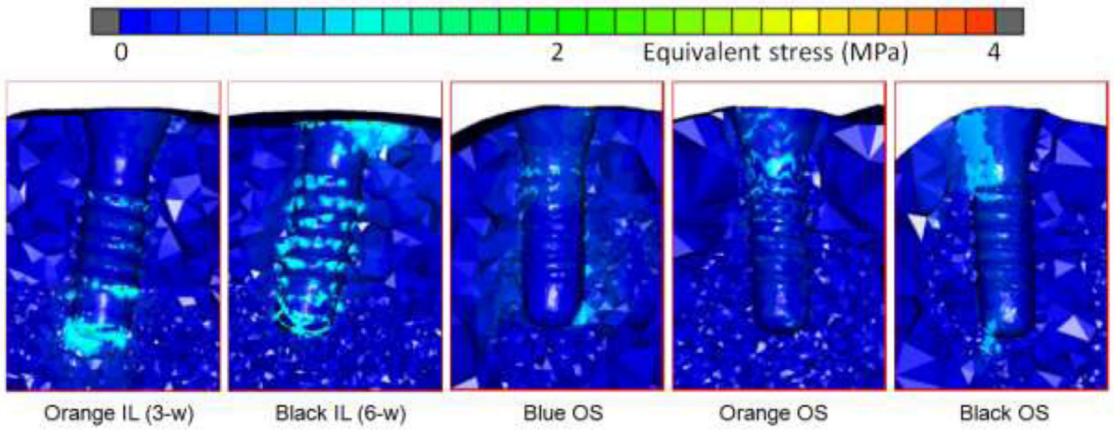

Fig. 5. Stresses distributions in the antler tissue for IL-models and OS-models. Orange IL (3-w): model of orange antler with immediately loaded implant for 3 weeks; black IL (6-w): model of black antler with immediately loaded implant for 6 weeks; blue OS: model of blue antler with unloaded implant; orange OS: model of orange antler with unloaded implant; black OS: model of black antler with unloaded implant.

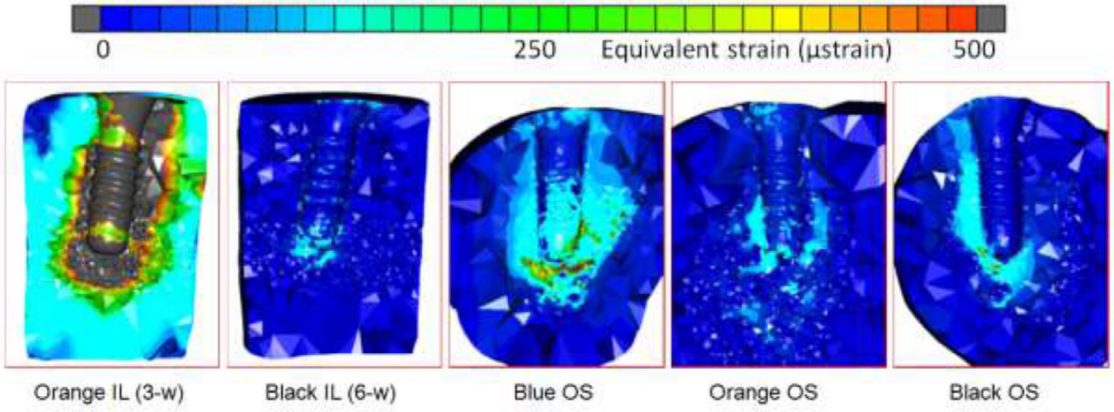

Fig. 6. Strains distributions in the antler tissue for IL-models and OS-models. Orange IL (3-w): model of orange antler with immediately loaded implant for 3 weeks; black IL (6-w): model of black antler with immediately loaded implant for 6 weeks; blue OS: model of blue antler with unloaded implant; orange OS: model of orange antler with unloaded implant; black OS: the model of black antler with unloaded implant.

Please cite this article as: Y. He et al., Biomechanical characteristics of immediately loaded and osseointegration dental implants inserted into Sika deer antler, Medical Engineering and Physics (2018), https://doi.org/10.1016/j.medengphy.2018.04.021

Table 6
Obtained maximum values of strains (μstrain) in antler tissue in osseointegrated (OS) and immediate loading (IL) models with different postoperative time.

	IL group	OS group	*t*	*P* value
Blue (2-week)		1888 ± 171		
Orange (3-week)	9879 ± 1965	686 ± 58[a]	14.9	<0.001
Black (6-week)	363 ± 81	523 ± 48[a,b]	−5.6	<0.001
F/*t*	15.3	479.0	–	–
P value	<0.001	<0.001		

[a] $P < 0.05$, when compared with blue.
[b] $P < 0.05$, when compared with orange.

formation [23]. An optimal bone response to immediately or early loaded implants is not only determined by the primary stability of the implant and the host bone characteristics, but also by the individual loading parameters and an optimized load transfer through appropriate implant design and surface features [24,25]. In order to observe the benefit of IL implants, considerations should be made regarding the mechanical behavior of the bone under loading conditions through appropriate numerical and experimental studies for optimizing the initial stability of the implants and subsequently their long-term success.

In the present study, controlled loading was immediately applied on implants inserted into Sika deer antlers. At the same time, implants without loading were investigated as well as a control group. The results indicated that BMD and Young's modulus of antler tissue around IL implants significantly increased as the loading time increased. This is due to the reason that well-controlled IL accelerates tissue mineralization at the peri-implant bone [5]. After shedding the antler, the BMD and Young's modulus of antler tissue remained in a similar value in all specimens, including specimens with implant and specimens without implant. These values were consistent with the results of the study by Chen et al. [26], who discovered that compact bone and cancellous bone density of deer antler were 1.72 g/cm^3 and 0.50 g/cm^3 and total bone density of the antler was 1.35 g/cm^3. Moreover, the results indicated that implants inserted into Sika deer antler might not disturb the growth and calcification process of antler.

Furthermore, there was a highly interesting result that in black antler, the BMD of antler tissue around the IL implant (2.00 g/cm^3) was much higher than that around the OS implant (1.30 g/cm^3). This indicates that the density of antler tissue around the implant increases over the loading period. However the density might be reduced after the complete osseointegration of the implant as shown in previous studies [27,28].

The existing studies relating to changes in bone density around IL implants concluded various results due to the different case selection, methods of measurement, and observation times. Lahori et al. [29] evaluated the changes in periimplant bone quality for mandibular implant-supported overdentures with ball attachments using delayed and immediate loading protocols. They concluded that bone density significantly increased for both groups at all time intervals (3, 6, 12 months) and the bone density in delayed loading group illustrated higher values than that in immediate loading group. However, Hasan et al. [30] evaluated the change in bone density of 20 individual immediately loaded implants by measuring the grey values of cone beam computed tomography (CBCT) at different periods subsequent to implant insertion and observed a reduction in grey values with respect to reference values after one month and six months from implant insertion in the apical, middle, and cervical regions.

The finite element method is a numerical method which is suitable for analyzing complex structures. This method was applied mostly in biomechanical studies of dental implants and peri-implant tissues by many researchers. The validity of the simulations depends on morphology, material properties, boundary conditions, and bone-implant interface. The most important input factors are material properties of implant and surrounding tissue, such as Young's modulus and Poisson's ratio [31]. Moreover, the geometry and architecture of bone are important factors for the finite element model as well. Since the complex spongious pattern is difficult to create, spongious bone network is not considered in most FEA analyses. It was mostly assumed that spongious bone as a homogenous core surrounded by a cortical layer. Since spongious bone architecture and its density can vary among species and anatomical locations within the same individual, it is difficult to present precise results from these simplified models and validate them with clinical data. With the development of microcomputed tomography and improved performance of analytical systems, it is currently possible to conduct biomechanical analysis, taking into consideration the actual morphology and structure of spongious bone. In the present study, finite element models with spongious bone microstructure were constructed from the μCT data and Young's modulus of antler tissue was calculated from the specimens. Moreover, implants subjected to immediate loading are in frictional contact with bone, which is responsible for their primary stability. Therefore, frictional contact was simulated in this study by using a frictional contact coefficient ($\mu = 0.3$) at the bone-implant interface [32,33]. Osseointegrated condition was simulated by defining perfect bonding interface between the bone and implant [34]. The above mentioned methods enabled the models to imitate the real situation as much as possible.

The results of this study showed that the maximum values of displacement and stress in implant and stress and strain in antler tissue were significantly different among OS models. This might be attributed to the various densities and geometries of antler tissue in different animals. In OS models with higher BMD and Young's modulus, strains in antler tissue were lower. This is due to the reason that the deformation of the bone tissue by means of strain is inversely correlated to its stiffness. The higher the strain value, the lower the stiffness of the bone.

Comparing the orange antler models, all the biomechanical results of IL model were significantly higher than those of orange antler OS model ($P < 0.05$) and wider distributions were obtained from IL models. Conversely, for black antler models, the displacements in implant and strains in antler tissue of IL model were significantly lower than OS model ($P < 0.05$) and narrower distribution of strains were detected in IL model. Theoretically, IL models should indicate higher biomechanical results, because only compressive and frictional forces are transferred via the contacting interfaces, compared with the bonded interfaces of the OS models. However, the models constructed in this study were from various specimens, and the biomechanical values can be influenced by the density of antler tissue, the geometry of antler tissue and contact condition of bone-implant interface. The considerably higher density of antler tissue in black antler IL model might be a reason for these results.

There were limitations in this study. First, the limited numbers of animal specimens, only three pairs of antlers were collected after their shedding due to the fact that it was difficult to find all the shedded antlers in a spacious activity place for Sika deer. Secondly, an empirical equation was used to calculate Young's modulus of antler tissue from BMD. However, this study provided theoretical foundation for developing the deer antler as a novel model for dental implant investigation.

5. Conclusions

After shedding the antler, the BMD of antler tissue in specimens with osseointegrated implants and without implants remained in

Please cite this article as: Y. He et al., Biomechanical characteristics of immediately loaded and osseointegration dental implants inserted into Sika deer antler, Medical Engineering and Physics (2018), https://doi.org/10.1016/j.medengphy.2018.04.021

a similar range. Implants inserted into Sika deer antler do not disturb the growth and calcification process of antler.

Density of antler tissue around the implant go up to relatively higher values after under immediate loading for a longer time period and the density might be reduced after osseointegration of the implant.

The biomechanical values are influenced by the density of antler tissue, the geometry of antler tissue and contact conditions of the bone-implant interface.

Funding

This investigation was supported by Straumann GmbH (Freiburg, Germany) and grants from National Natural Science Foundation of China (11702231). The study sponsors have no involvement in the study design, in the collection, analysis and interpretation of data, in the writing of the manuscript, or in the decision to submit the manuscript for publication.

Conflict of interest

The authors declare that there is no conflict of interest.

Acknowledgments

The authors thank the staff of Raptor Center and Wildlife Parc Hellenthal, especially Mr. Joerg Niesters, Mr. Karl Fischer, Mr. Dirk Wynands and Dr. Martin Boettcher for care of the animals, thank the staff of Endowed Chair of Oral Technology, University of Bonn, Dr. Susanne Reimann and Ms. Anna Weber for preparing and scanning the specimens by μCT scanner, and thank Mr. Tim Klunter for taking out the specimens from antlers.

References

[1] Albrektsson T, Brånemark PI, Hansson HA, Lindström J. Osseointegrated titanium implants. Requirements for ensuring a long-lasting, direct bone-implant anchorage in man. Acta Orthop Scand 1981;52:155–70.
[2] Albrektsson T, Johansson C. Osteoinduction, osteoconduction andosseointegration. Eur Spine J 2001;10(Suppl 2):S96–S101.
[3] Joos U, Meyer U. New paradigm in implant osseointegration. Head FaceMed 2006;2:19.
[4] Camargos GV, Sotto-Maior BS, Silva WJ, Lazari PC, Del Bel Cury AA. Prosthetic abutment influences bone biomechanical behavior of immediately loaded implants. Braz Oral Res 2016;30:1–9.
[5] Duyck J, Vandamme K. The effect of loading on peri-implant bone: a critical review of the literature. J Oral Rehabil 2014;41:783–94.
[6] Romanos GE. Biomolecular cell-signaling mechanisms and dental implants: a review on the regulatory molecular biologic patterns under functional and immediate loading. Int J Oral Maxillofac Implants 2016;31:939–51.
[7] Melilli D, Rallo A, Cassaro A. Implant overdentures: recommendations and analysis of the clinical benefits. Minerva Stomatol 2011;60:251–69.
[8] Pearce AI, Richards RG, Milz S, Schneider E, Pearce SG. Animal models for implant biomaterial research in bone: a review. Eur Cell Mater 2007;13:1–10.
[9] Schimandle JH, Boden SD. Spine update. The use of animal models to study spinal fusion. Spine 1994;19:1998–2006.
[10] Li C, Zhao H, Liu Z, McMahon C. Deer antler-a novel model for studying organ regeneration in mammals. Int J Biochem Cell Biol 2014;56:111–22.
[11] Goss RJ. Future directions in antler research. Anat Rec 1995;241:291–302.
[12] Li C, Suttie JM. Tissue collection methods for antler research. Eur J Morphol 2003;41:23–30.
[13] Currey JD, Landete-Castillejos T, Estevez J, Ceacero F, Olguin A, Garcia A, Gallego L. The mechanical properties of red deer antler bone when used in fighting. J Exp Biol 2009;212:3985–93.
[14] Rolf HJ, Enderle A. Hard fallow deer antler: a living bone till antler casting? Anat Rec 1999;255:69–77.
[15] Kierdorf U, Stoffels E, Stoffels D, Kierdorf H, Szuwart T, Clemen G. Histological studies of bone formation during pedicle restoration and early antler regeneration in roe deer and fallow deer. Anat Rec A Discov Mol Cell Evol Biol 2003;273:741–51.
[16] Li C, Suttie JM, Clark DE. Histological examination of antler regeneration in red deer (Cervus elaphus). Anat Rec A Discov Mol Cell Evol Biol 2005;282:163–74.
[17] Caulkett N, Haigh JC. Deer (Cervids). In: West G, Heard D, Caulkett N, editors. Zoo animal and wildlife immobilization and anaesthesia. Ames Iowa: Blackwell Publishing; 2007. p. 607–12.
[18] Wiesner H, von Hegel G. Practical advice concerning the immobilization of wild and zoo animals. Tierarztl Prax 1985;13:113–27.
[19] Rahimi A, Klein R, Keilig L, Abboud M, Wahl G, Bourauel C. Development and design of a novel loading device for the investigation of bone adaptation around immediately loaded dental implants using the reindeer antler as implant bed. J Biomech 2009;42:2415–18.
[20] Beaupré GS, Orr TE, Carter DR. An approach for time-dependent bone modeling and remodeling-theoretical development. J Orthop Res 1990;8:651–61.
[21] Gottlow J, Dard M, Kjellson F, Obrecht M, Sennerby L. Evaluation of a new titanium-zirconium dental implant: a biomechanical and histological comparative study in the mini pig. Clin Implant Dent Relat Res 2012;14:538–45.
[22] Webster D, Schulte FA, Lambers FM, Kuhn G, Müller R. Strain energy density gradients in bone marrow predict osteoblast and osteoclast activity: a finite element study. J Biomech 2015;48:866–74.
[23] Balaji P, Balaji SM, Ugandhar P. Immediate implant in single rooted teeth – study on primary stability and bone formation. Indian J Dent Res 2015;26:421–6.
[24] Götz W, Gedrange T, Bourauel C, Hasan I. Clinical, biomechanical and biological aspects of immediately loaded dental implants: a critical review of the literature. Biomed Techol 2010;55:311–15.
[25] Schnitman PA, Hwang JW. To immediately load, expose, or submerge in partial edentulism: a study of primary stability and treatment outcome. Int J Oral Maxillofac Implants 2011;26:850–9.
[26] Chen PY, Stokes AG, McKittrick J. Comparison of the structure and mechanical properties of bovine femur bone and antler of the North American elk (Cervus elaphus canadensis). Acta Biomater 2009;5:693–706.
[27] Ramachandran A, Singh K, Rao J, Mishra N, Jurel SK, Agrawal KK. Changes in alveolar bone density around immediate functionally and nonfunctionally loaded implants. J Prosthet Dent 2016;115:712–17.
[28] Mainetti T, Lang NP, Bengazi F, Sbricoli L, Soto Cantero L, Botticelli D. Immediate loading of implants installed in a healed alveolar bony ridge or immediately after tooth extraction: an experimental study in dogs. Clin Oral Implants Res 2015;26:435–41.
[29] Lahori M, Kaul AS, Chandra S, Nagrath R, Gupta H. Comparative evaluation of bone in mandibular implant retained overdentures using delayed and immediate loading protocol: an in-vivo study. J Indian Prosthodont Soc 2013;13:113–21.
[30] Hasan I, Dominiak M, Blaszczyszyn A, Bourauel C, Gedrange T, Heinemann F. Radiographic evaluation of bone density around immediately loaded implants. Ann Anat 2015;199:52–7.
[31] Seker E, Ulusoy M, Ozan O, DÖ Doğan, Seker BK. Biomechanical effects of different fixed partial denture designs planned on bicortically anchored short, graft-supported long, or 45-degree-inclined long implants in the posterior maxilla: a three-dimensional finite element analysis. Int J Oral Maxillofac Implants 2014;29:e1–9.
[32] Hasan I, Keilig L, Staat M, Wahl G, Bourauel C. Determination of the frictional coefficient of the implant-antler interface: experimental approach. Biomed Technol 2012;57:359–63.
[33] Huang HL, Hsu JT, Fuh LJ, Tu MG, Ko CC, Shen YW. Bone stress and interfacial sliding analysis of implant designs on an immediately loaded maxillary implant: a non-linear finite element study. J Dent 2008;36:409–17.
[34] Murakami N, Wakabayashi N. Finite element contact analysis as a critical technique in dental biomechanics: a review. J Prosthodont Res 2014;58:92–101.